IEEE Access
Multidisciplinary : Rapid Review : Open Access Journal

Received 10 September 2024, accepted 2 October 2024, date of publication 7 October 2024, date of current version 18 October 2024.
Digital Object Identifier 10.1109/ACCESS.2024.3474801

RESEARCH ARTICLE

Embedding Classic Chaotic Maps in Simple Discrete-Time Memristor Circuits

MAURO DI MARCO[1], **MAURO FORTI**[1], **LUCA PANCIONI**[1], **GIACOMO INNOCENTI**[2], **AND ALBERTO TESI**[2]
[1]Department of Information Engineering and Mathematics, University of Siena, 53100 Siena, Italy
[2]Department of Information Engineering, University of Florence, 50139 Florence, Italy
Corresponding author: Mauro Forti (forti@dii.unisi.it)

ABSTRACT In the last few years the literature has witnessed a remarkable surge of interest for maps implemented by discrete-time (DT) memristor circuits. One main reason is that from numerical simulations it appears that even for simple memristor circuits the maps can easily display complex dynamics, including chaos and hyperchaos, which are of relevant interest for engineering applications. Goal of this manuscript is to investigate on the reasons underlying this type of complex behavior. To this end, the manuscript considers the map implemented by the simplest memristor circuit given by a capacitor and an ideal flux-controlled memristor or an inductor and an ideal charge-controlled memristor. In particular, the manuscript uses the DT flux-charge analysis method (FCAM) introduced in a recent paper to ensure that the first integrals and foliation in invariant manifolds of continuous-time (CT) memristor circuits are preserved exactly in the discretization for any step size. DT-FCAM yields a two-dimensional map in the voltage-current domain (VCD) and a manifold-dependent one-dimensional map in the flux-charge domain (FCD), i.e., a one-dimensional map on each invariant manifold. One main result is that, for suitable choices of the circuit parameters and memristor nonlinearities, both DT circuits can exactly embed two classic chaotic maps, i.e., the logistic map and the tent map. Moreover, due to the property of extreme multistability, the DT circuits can simultaneously embed in the manifolds all the dynamics displayed by varying one parameter in the logistic and tent map. The paper then considers a DT memristor Murali-Lakshmanan-Chua circuit and its dual. Via DT-FCAM these circuits implement a three-dimensional map in the VCD and a two-dimensional map on each invariant manifold in the FCD. It is shown that both circuits can simultaneously embed in the manifolds all the dynamics displayed by two other classic chaotic maps, i.e., the Hénon map and the Lozi map, when varying one parameter in such maps. In essence, these results provide an explanation of why it is not surprising to observe complex dynamics even in simple DT memristor circuits.

INDEX TERMS Chaos, discrete-time circuits, extreme multistability, first integral, flux-charge analysis method, Hénon map, invariant manifold, logistic map, memristor circuit.

I. INTRODUCTION

Memristor has been theoretically envisioned by Leon Chua in a seminal paper published in 1971 [1] as the fourth basic passive circuit element in addition to resistor, capacitor and inductor. More than thirty years later, in 2007, a team at HP led by Stanley Williams made the fundamental discovery that we can physically observe memristive behavior in some metal-insulator-metal (MIM) solid-state devices [2]. This discovery has triggered an unprecedented and widespread interest in the theory and applications of continuous-time (CT) circuits with memristors, memcapacitors and meminductors [3], [4], [5], [6], [7], [8], [9], [11], [12]. Among the many relevant potential applications there are the implementation of high-density and low power random access memories [13], [14], [15]. More generally, the memristor is seen as a strategic component for implementing in-memory computing schemes, akin to the computation mechanism

The associate editor coordinating the review of this manuscript and approving it for publication was Leimin Wang.

of the brain, aiming at overcoming basic limitations of traditional Von Neumann computing machines [16], [17], [18], [19], [20], [21], [22].

Recent years have witnessed a significant surge of interest also for discrete time (DT) versions of memristor circuits. During a first phase, Euler's discretization method has been employed to derive discrete memristor models [23] and to study the discretization of simple CT memristor circuits [24]. Subsequent studies have also investigated more abstract maps employing typical memristor nonlinearities but not necessarily related to the discretization of a CT counterpart [25], [26], [27], [28], [29]. There are strong motivations for considering DT memristor circuits. First of all, since solid-state memristors are not easily available as yet, DT emulators can be useful to assess their performance without relying on experimental measurements. Moreover, DT memristor circuits can be easily and effectively interfaced with digital computers. However, the most relevant motivation is maybe that maps of DT memristor circuits can easily generate complex dynamics that are of interest in themselves for engineering applications. The main dynamical aspects studied in the literature include, but are not limited to, chaos and hyperchaos displayed by DT memristor maps [26], [28], [29], [30], [31], [32], [33], [34], [35], [36], [37], [38] and coexisting attractors, multistability and extreme multistability in memristor circuits with special classes of memristor nonlinearities [40], [41], [42]. The generated complex dynamics have found relevant applications in the fields of random number generation [32], [43], secure communications [31], [44], implementation of reservoir computing systems [45], [46] and biomedical image encryption [47], [48], [49].

A recent line of research has addressed the extension to DT memristor circuits of the flux-charge analysis method (FCAM), a technique that was originally developed for CT memristor circuits [6], [50]. In particular, the paper [51] has introduced a special discretization scheme ensuring that the first integrals of CT memristor circuits are exactly preserved in the discretization for any step size. As a consequence, the state space in the voltage-current domain (VCD) of DT memristor circuits can be foliated in invariant manifolds and on each manifold the circuits obey a manifold-dependent reduced-order dynamics in the flux-charge domain (FCD). Such a structural property gives a rigorous explanation of the so-called extreme multistability property of DT memristor circuits, i.e., the coexistence of infinitely many different dynamics and attractors for a fixed set of circuit parameters.

An inspection of the literature shows that even relatively simple DT memristor circuits can easily display really complex dynamics including chaos and hyperchaos [52], [53]. It is then natural to ask if we can find a rationale for this kind of behavior. Goal of this manuscript is to give an answer to this question via the study of the maps implemented via DT-FCAM by a simple DT memristor-capacitor circuit and a DT Murali-Lakshmanan-Chua circuit [54]. It is shown that, by a suitable choice of the memristor nonlinearity and circuit parameters, such circuits can embed, as a manifold-dependent reduced-order dynamics in the FCD, a number of classic chaotic maps, namely, the *logistic and the tent map as well as the Hénon and Lozi map* [55], [56]. Another particularly intriguing feature is that by varying the manifold the *memristor circuits can embed all the dynamics that are generated by varying one parameter in the logistic or Hénon map.* This represents an effective way to exploit the property of coexisting attractors and extreme multistability, which is peculiar to DT memristor circuits [51]. In overall, the obtained results clearly show why it is not surprising to observe complex dynamics even in simple DT memristor circuits.

The organization of the manuscript can be outlined as follows. Sect. II first summarizes some results from DT-FCAM needed in the manuscript and then it derives the maps implemented by the considered classes of DT memristor circuits. Thereafter, Sect. III and Sect. IV show how the logistic, tent, Hénon and Lozi maps can be embedded in the DT memristor circuits. Finally, the main conclusions in the paper are given in Sect. V.

II. TWO SIMPLE CLASSES OF DT MEMRISTOR CIRCUITS

One basic question in dynamic system theory is whether it is possible to embed the dynamics of a given system into a higher-order system with a given structure. One relevant and quite unexpected result in this sense has been obtained by Stephen Smale in [57] for CT systems. In that paper it is shown that any n-th order CT dynamics can be embedded in a CT competitive system of order $n+1$. More precisely, Smale devised a suitable design procedure ensuring that any given n-th order CT dynamics evolves on an attracting n-th order invariant manifold of the $(n+1)$-th order CT competitive system. One problem however is that the equations of the embedding system do not resemble those of a network. More details on the construction of the embedding competitive system can be found in [57]. An analogous result holds for CT cooperative systems, although in this case the n-th order manifold is a repelling one [58]. As discussed in [59, Sect. 11], this follows since a CT irreducible cooperative system is such that almost all its solutions converge to the set of equilibria. More recently, in [60] it has been shown how CT memristor circuits can embed the FitzHugh-Nagumo system [61] and the Duffing oscillators [62].

In this manuscript, we address an embedding problem for a class of maps implemented by DT memristor circuits obtained via DT-FCAM [51]. More specifically, we study if it is possible to embed the logistic and the tent map, which are one-dimensional maps, as reduced-order dynamics in the invariant manifolds of a two-dimensional DT flux-controlled memristor and capacitor circuit or its dual (a charge-controlled memristor and inductor circuit). Moreover, we investigate whether we can embed the Hénon and the Lozi map, which are two-dimensional maps, as reduced-order dynamics in the invariant manifolds of a three-dimensional

DT Murali-Lakshmanan-Chua or its dual. First of all, in the remaining part of this section, we recall some basic facts on DT-FCAM useful for the analysis in the paper. Then, in Sect. II-B and Sect. II-C, we derive the maps implemented in the VCD and FCD by the considered classes of DT memristor circuits.

A. ANALYSIS VIA DT-FCAM

FCAM has been developed in [50] and [63] (see also the general treatment in [6]) to analyze a class of CT circuits containing ideal resistors, capacitors, inductors and ideal flux-controlled or charge-controlled memristors. The method is based on analyzing the circuits both in the standard voltage current domain (VCD) and in the flux-charge domain (FCD) using Kirchhoff laws and constitutive relations of circuit elements. One relevant result obtained via FCAM is that for structural reasons a CT memristor circuit possesses first integrals in the VCD. Hence, the state space is foliated in invariant manifolds where the circuit satisfies a manifold-dependent reduced-order dynamics in the FCD. Later on, the recent article [51] has extended FCAM to DT memristor circuits. At the basis of DT-FCAM is the use of a special discretization scheme for the memristor circuits ensuring that the first integrals are exactly preserved in the discretization for any step size. This ensures that also a DT memristor circuit possesses integrals of motion and, as a consequence, its state space is foliated in invariant manifolds.

Consider a two-terminal element (a one-port) with voltage v and current i. Let $\varphi(t) = \int_{-\infty}^{t} v(\tau)d\tau$ and $q(t) = \int_{-\infty}^{t} i(\tau)d\tau$ be the flux and charge, respectively. Moreover, consider the incremental flux $\varphi^0(t) = \int_0^t v(\tau)d\tau$ and incremental charge $q^0(t) = \int_0^t i(\tau)d\tau$ [50]. Given the sampling instants $t_k = kh$, $k = 0, 1, 2, \ldots$, where $h > 0$ is the step size, the corresponding discretized electric quantities are given by $v_k = v(t_k)$, $i_k = i(t_k)$, $\varphi_k = \varphi(t_k)$, $q_k = q(t_k)$, $\varphi_k^0 = \varphi^0(t_k)$ and $q_k^0 = q^0(t_k)$.

In the VCD, Kirchhoff voltage law (KVL) can be expressed as $\sum_j v_{j,k} = 0$ around any loop, whereas Kirchhoff current law (KCL) is given as $\sum_j i_{j,k} = 0$ for any cut-set. In the FCD, Kirchhoff flux law (KφL) is given as $\sum_j \varphi_{j,k}^0 = 0$ around any loop, while Kirchhoff charge law (KqL) can be expressed as $\sum_j q_{j,k}^0 = 0$ for any cut-set [51].

Consider a linear capacitor $q_C = Cv_C$ or $i_C = Cdv_C/dt$. Via forward Euler rule we obtain the one-dimensional map (VCD)

$$i_{C,k} = C\frac{v_{C,k+1} - v_{C,k}}{h}. \tag{1}$$

Moreover, in the FCD the capacitor satisfies the one-dimensional map

$$q_{C,k}^0 = C\frac{\varphi_{C,k+1}^0 - \varphi_{C,k}^0}{h} - Cv_{C0} \tag{2}$$

where $v_{C0} = v_C(0)$.

Consider now a linear inductor $\varphi_L = Li_L$ or $v_L = Ldi_L/dt$. Applying forward Euler rule we obtain the one-dimensional map (VCD)

$$v_{L,k} = L\frac{i_{L,k+1} - i_{L,k}}{h}. \tag{3}$$

Moreover, in the FCD the inductor satisfies the one-dimensional map

$$\varphi_{L,k}^0 = L\frac{q_{L,k+1}^0 - q_{L,k}^0}{h} - Li_{L0} \tag{4}$$

where $i_{L0} = i_L(0)$

A flux-controlled memristor is defined by $q_M = \hat{q}(\varphi_M)$. This yields (VCD)

$$\begin{cases} i_M = \hat{q}'(\varphi_M)v_M \\ \dot{\varphi}_M = v_M. \end{cases} \tag{5}$$

In accordance with [51], we use for the memristor the discretization scheme (VCD)

$$\begin{cases} i_{M,k} = \dfrac{\hat{q}(\varphi_{M,k+1}) - \hat{q}(\varphi_{M,k})}{h} \\ \varphi_{M,k+1} = \varphi_{M,k} + hv_{M,k}. \end{cases} \tag{6}$$

On the other hand we have (FCD)

$$q_{M,k}^0 = \hat{q}(\varphi_{M,k}^0 + \varphi_{M0}) - \hat{q}(\varphi_{M0}) \tag{7}$$

where $\varphi_{M0} = \varphi_M(0)$.

A charge-controlled memristor is defined by $\varphi_M = \hat{\varphi}(q_M)$. This yields (VCD)

$$\begin{cases} v_M = \hat{\varphi}'(q_M)i_M \\ \dot{q}_M = i_M. \end{cases} \tag{8}$$

In accordance with [51], we use for the memristor the discretization scheme (VCD)

$$\begin{cases} v_{M,k} = \dfrac{\hat{\varphi}(q_{M,k+1}) - \hat{\varphi}(q_{M,k})}{h} \\ q_{M,k+1} = q_{M,k} + hi_{M,k}. \end{cases} \tag{9}$$

On the other hand we have (FCD)

$$\varphi_{M,k}^0 = \hat{\varphi}(q_{M,k}^0 + q_M(0)) - \hat{\varphi}(q_{M0}) \tag{10}$$

where $\varphi_{M0} = \varphi_M(0)$.

Remark 1: We stress that the discretization schemes for the memristor given in (6) and (9) guarantee that the first integrals of CT memristor circuits are preserved in the discretization for any step size [51]. As such, they basically differ from typical discretization schemes used in the literature that do not preserve first integrals [64]. ■

B. MC AND ML CIRCUITS

First, let us consider the MC circuit in Fig. 1(a) (VCD), which is composed of an ideal flux-controlled memristor and an ideal capacitor. The corresponding circuit in the FCD is shown in Fig. 1(b). The next result provides us with the maps implemented by the circuit in the VCD and FCD. It also gives the expression of the first integral and the invariant manifolds of the circuit.

Proposition 1: The following results hold:

1) In the VCD the dynamics of the MC circuit is described by the two-dimensional map in the state variables $v_{C,k}$ and $\varphi_{M,k}$

$$\begin{cases} v_{C,k+1} = v_{C,k} - \dfrac{1}{C}(\hat{q}(\varphi_{M,k} + hv_{C,k}) - \hat{q}(\varphi_{M,k})) \\ \varphi_{M,k+1} = \varphi_{M,k} + hv_{C,k}. \end{cases} \tag{11}$$

2) The function of the state variables given by

$$\Theta_{\mathrm{MC}}(v_C, \varphi_M) = Cv_C + \hat{q}(\varphi_M)$$

is a first integral of (11) for any step size h, i.e., we have $\Theta_{\mathrm{MC}}(v_{C,k+1}, \varphi_{M,k+1}) = \Theta_{\mathrm{MC}}(v_{C,k}, \varphi_{M,k})$, $k = 0, 1, 2, \ldots$.

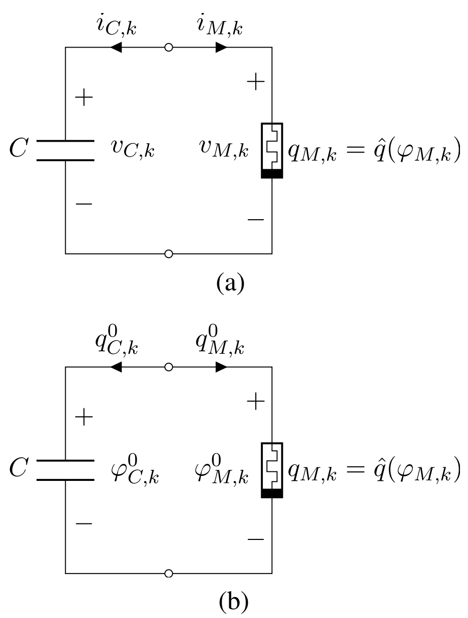

FIGURE 1. **DT MC circuit. (a) VCD and (b) FCD.**

3) The state space of (11) is foliated in one-dimensional invariant manifolds

$$\mathcal{M}_{\mathrm{MC}}(Q_0) = \{(v_C, \varphi_M) \in \mathbb{R}^2 : \\ \Theta_{\mathrm{MC}}(v_C, \varphi_M) = Cv_C + \hat{q}(\varphi_M) = Q_0\}$$

where $Q_0 \in \mathbb{R}$ is the manifold index. On each manifold, i.e., in the FCD, the dynamics is described by the one-dimensional map in the state variable $\varphi_{M,k}$

$$\varphi_{M,k+1} = \varphi_{M,k} - \frac{h}{C}\hat{q}(\varphi_{M,k}) + \frac{h}{C}Q_0. \tag{12}$$

■

Proof: 1) Let us show that in the VCD the dynamics of the MC circuit is described by the two-dimensional map

$$\begin{cases} v_{C,k+1} = v_{C,k} - \dfrac{1}{C}(\hat{q}(\varphi_{M,k} + hv_{C,k}) - \hat{q}(\varphi_{M,k})) \\ \varphi_{M,k+1} = \varphi_{M,k} + hv_{C,k}. \end{cases} \tag{13}$$

To this end, we perform the analysis of the DT circuit in Fig.1(a) using Kirchhoff laws and constitutive relations of circuit elements. KCL and KVL written for such a circuit yield

$$i_{C,k} + i_{M,k} = 0, \tag{14}$$

$$v_{C,k} = v_{M,k}. \tag{15}$$

Substituting the constitutive relation (1) and the first equation of (6) in (14) we obtain

$$C\frac{v_{C,k+1} - v_{C,k}}{h} + \frac{\hat{q}(\varphi_{Mk+1}) - \hat{q}(\varphi_{Mk})}{h} = 0 \tag{16}$$

while using (15) in the second equation of (6) allows us to write

$$\varphi_{M,k+1} = \varphi_{M,k} + hv_{C,k} \tag{17}$$

i.e., the second equation of (13). Substituting (17) into (16), after simple algebraic manipulation we obtain

$$v_{C,k+1} = v_{C,k} - \frac{1}{C}(\hat{q}(\varphi_{M,k} + hv_{C,k}) - \hat{q}(\varphi_{M,k}))$$

i.e., the first equation of (13), thus completing the proof of the statement.

2) Follows directly by reordering the terms of (16).

3) From (16) we have that, for any $k \geq 1$,

$$Cv_{C,k} + \hat{q}(\varphi_{M,k}) = Cv_{C,0} + \hat{q}(\varphi_{M,0}) = Q_0$$

i.e., the state variables are bound to evolve on the manifold $\mathcal{M}_{\mathrm{MC}}(Q_0)$. To derive the equations describing the dynamics on $\mathcal{M}_{\mathrm{MC}}(Q_0)$, let us write the K$q$L and K$\varphi$L for the MC circuit in Fig. 1(b)

$$q^0_{C,k} + q^0_{M,k} = 0 \tag{18}$$

$$\varphi^0_{C,k} = \varphi^0_{M,k}. \tag{19}$$

Substituting (2) and (7) in (18) we obtain

$$C\frac{\varphi^0_{C,k+1} - \varphi^0_{C,k}}{h} - Cv_{C,0} \\ + \hat{q}(\varphi^0_{M,k} + \varphi_{M,0}) - \hat{q}(\varphi_{M,0}) = 0.$$

Considering (19), we obtain

$$\varphi^0_{M,k+1} = \varphi^0_{M,k} - \frac{h}{C}\hat{q}(\varphi^0_{M,k} + \varphi_{M,0}) + hv_{C,0} + \frac{h}{C}\hat{q}(\varphi_{M,0})$$

which can be recast into (12) by summing $\varphi_{M,0}$ to both sides and taking into account the expression of Q_0. ■

Now, let us consider the dual of the circuit in Fig. 1, which is composed of an ideal charge-controlled memristor and an ideal inductor, as depicted in Fig. 2(a) (VCD). The corresponding circuit in the FCD is shown in Fig. 2(b).

Proposition 2: The following results hold:

1) In the VCD the dynamics of the ML circuit is described by the two-dimensional map in the state variables $i_{L,k}$ and $q_{M,k}$

$$\begin{cases} i_{L,k+1} = i_{L,k} - \dfrac{1}{L}(\hat{\varphi}(q_{M,k} + hi_{L,k}) - \hat{\varphi}(q_{M,k})) \\ q_{M,k+1} = q_{M,k} + hi_{L,k}. \end{cases} \tag{20}$$

2) The function of the state variables given by

$$\Theta_{\mathrm{ML}}(i_L, q_M) = Li_L + \hat{\varphi}(q_M)$$

is a first integral of (20) for any step size h, i.e., we have $\Theta_{\mathrm{ML}}(i_{L,k+1}, q_{M,k+1}) = \Theta_{\mathrm{ML}}(i_{L,k}, q_{M,k})$, $k = 0, 1, 2, \ldots$.

3) The state space of (20) is foliated in one-dimensional invariant manifolds

$$\mathcal{M}_{\mathrm{ML}}(\Phi_0) = \{(i_L, q_M) \in \mathbb{R}^2 : \Theta_{\mathrm{ML}}(i_L, q_M) = Li_L + \hat{\varphi}(q_M) = \Phi_0\}$$

where $\Phi_0 \in \mathbb{R}$ is the manifold index. On each manifold, i.e., in the FCD, the dynamics is described by the one-dimensional map in the state variable $q_{M,k}$

$$q_{M,k+1} = q_{M,k} - \frac{h}{L}\hat{\varphi}(q_{M,k}) + \frac{h}{L}\Phi_0. \tag{21}$$

■

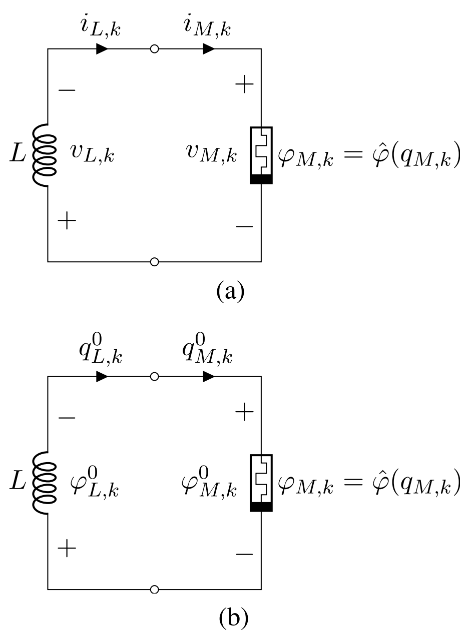

FIGURE 2. **DT ML circuit. (a) VCD and (b) FCD.**

Proof: 1) Let us show that the dynamics in the VCD of the ML circuit is described by the two-dimensional map

$$\begin{cases} i_{L,k+1} = i_{L,k} - \dfrac{1}{L}(\hat{\varphi}(q_{M,k} + hi_{L,k}) - \hat{\varphi}(q_{M,k})) \\ q_{M,k+1} = q_{M,k} + hi_{L,k}. \end{cases} \tag{22}$$

To this end, we perform the analysis of the DT circuit in Fig.2(a) using Kirchhoff laws and constitutive relations of circuit elements. KCL and KVL written for such a circuit yield

$$v_{L,k} + v_{M,k} = 0 \tag{23}$$
$$i_{L,k} = i_{M,k}. \tag{24}$$

Substituting the constitutive relation (3) and the first equation of (9) in (23) we obtain

$$L\frac{i_{L,k+1} - i_{L,k}}{h} + \frac{\hat{\varphi}(q_{Mk+1}) - \hat{\varphi}(q_{Mk})}{h} = 0 \tag{25}$$

while using (24) in the second equation of (9) permits to write

$$q_{M,k+1} = q_{M,k} + hi_{L,k} \tag{26}$$

i.e., the second equation of (20). Substituting (26) into (25), after simple algebraic manipulation we obtain

$$i_{L,k+1} = i_{L,k} - \frac{1}{L}(\hat{\varphi}(q_{M,k} + hi_{L,k}) - \hat{\varphi}(q_{M,k}))$$

i.e., the first equation of (20), thus completing the proof of the statement.

2) Follows directly by reordering the terms of (25).

3) From (25) we have that, for any $k > 1$,

$$Li_{L,k} + \hat{\varphi}(q_{M,k}) = Li_{L,0} + \hat{\varphi}(q_{M,0}) = \Phi_0$$

i.e., the state variables are bound to evolve on the manifold $\mathcal{M}_{\mathrm{ML}}(\Phi_0)$. To derive the equations describing the dynamics on such a manifold, let us first write the KqL and KφL for the ML circuit in Fig. 2(b)

$$q^0_{L,k} = q^0_{M,k} \tag{27}$$
$$\varphi^0_{L,k} + \varphi^0_{M,k} = 0. \tag{28}$$

Substituting (4) and (10) in (28) we obtain

$$L\frac{q^0_{L,k+1} - q^0_{L,k}}{h} - Li_{L,0} + \hat{\varphi}(q^0_{M,k} + q_{M,0}) - \hat{\varphi}(q_{M,0}) = 0.$$

Considering (27), we have

$$q^0_{M,k+1} = q^0_{M,k} - \frac{h}{L}\hat{\varphi}(q^0_{M,k} + q_{M,0}) + hi_{L,0} + \frac{h}{L}\hat{\varphi}(q_{M,0})$$

which can be recast into (21) by summing $q_{M,0}$ to both sides and taking into account the expression of Φ_0. ■

Clearly, via a suitable change of variables, it is possible to put the maps, first integral and invariant manifolds of the MC circuit and its dual in the same abstract mathematical form. Indeed, for the MC circuit, let $x_k = \varphi_{M,k}$, $y_k = v_{C,k}$, $\delta = 1/C$, $F(\cdot) = \hat{q}(\cdot)$ and $I_0 = Q_0$. Moreover, for the ML circuit, let $x_k = q_{M,k}$, $y_k = i_{L,k}$, $\delta = 1/L$, $F(\cdot) = \hat{\varphi}(\cdot)$ and $I_0 = \Phi_0$. Then, for both circuits the dynamics in the VCD obeys the two-dimensional map in the state variables x_k and y_k

$$\begin{cases} y_{k+1} = y_k - \delta(F(x_k + hy_k) - F(x_k)) \\ x_{k+1} = x_k + hy_k. \end{cases} \tag{29}$$

Moreover, there exists a first integral given by

$$\Theta(x, y) = \frac{1}{\delta}y + F(x) \tag{30}$$

and the state space in the VCD is foliated in the invariant manifolds

$$\mathcal{M}(I_0) = \{(x, y) \in \mathbb{R}^2 : \Theta(x, y) = \frac{1}{\delta}y + F(x) = I_0\}$$

where $I_0 \in \mathbb{R}$ is the manifold index. On each manifold the dynamics is described in the FCD by the one-dimensional map in the state variable x_k

$$x_{k+1} = x_k - h\delta F(x_k) + h\delta I_0. \tag{31}$$

C. MEMRISTOR MURALI-LAKSHMANAN-CHUA CIRCUIT AND ITS DUAL

Fig. 3(a) depicts a circuit in the VCD, obtained from Murali-Lakshmanan-Chua (MLC) circuit by replacing the nonlinear resistor with a flux-controlled memristor [54], [60], [65], [66]. For more generality, a voltage-controlled voltage-source (VCVS) is also added in series with the inductor. The corresponding circuit in the FCD is shown in Fig. 3(b). The MLC circuit is a simplified version of the celebrated Chua's circuit [67].

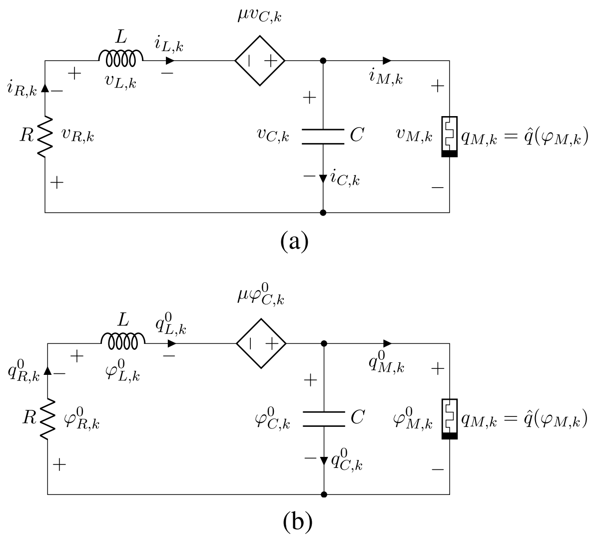

FIGURE 3. DT MLC circuit. (a) VCD and (b) FCD.

Proposition 3: The following results hold:

1) In the VCD the dynamics of MLC circuit is described by the three-dimensional map in the state variables $v_{C,k}$, $i_{L,k}$ and $\varphi_{M,k}$

$$\begin{cases} v_{C,k+1} = v_{C,k} - \dfrac{\hat{q}(\varphi_{M,k} + hv_{C,k}) - \hat{q}(\varphi_{M,k})}{C} + \dfrac{h}{C} i_{L,k} \\ i_{L,k+1} = (1 - \dfrac{Rh}{L}) i_{L,k} + \dfrac{h}{L}(\mu - 1) v_{C,k} \\ \varphi_{M,k+1} = \varphi_{M,k} + hv_{C,k}. \end{cases} \tag{32}$$

2) The function of the state variables given by

$$\Theta_{\mathrm{MLC}}(v_C, i_L, \varphi_M) = Cv_C + \frac{Li_L}{R} + \hat{q}(\varphi_M) + \frac{1-\mu}{R}\varphi_M$$

is a first integral of (32) for any step size h, i.e., we have $\Theta_{\mathrm{MLC}}(v_{C,k+1}, i_{L,k+1}, \varphi_{M,k+1}) = \Theta_{\mathrm{MLC}}(v_{C,k}, i_{L,k}, \varphi_{M,k})$, $k = 0, 1, 2, \ldots$.

3) The state space of (32) is foliated in two-dimensional invariant manifolds

$$\mathcal{M}_{\mathrm{MLC}}(Q_0) = \{(v_C, i_L, \varphi_M) \in \mathbb{R}^3 : \Theta_{\mathrm{MLC}}(v_C, i_L, \varphi_M) = Cv_C + \frac{Li_L}{R} + \hat{q}(\varphi_M) + \frac{1-\mu}{R}\varphi_M = Q_0\}$$

where $Q_0 \in \mathbb{R}$ is the manifold index. On each manifold, i.e., in the FCD, the dynamics is described by the two-dimensional map in the state variables $\varphi_{M,k}$ and $y_k = q^0_{L,k} + \frac{\mu-1}{R}\varphi_{M,0} - \frac{L}{R} i_{L,0}$

$$\begin{cases} \varphi_{M,k+1} = \varphi_{M,k} + \dfrac{h}{C} y_k - \dfrac{h}{C}\hat{q}(\varphi_{M,k}) + \dfrac{h}{C} Q_0 \\ y_{k+1} = (1 - \dfrac{hR}{L}) y_k + \dfrac{h}{L}(\mu - 1)\varphi_{M,k}. \end{cases} \tag{33}$$

■

Proof: 1) First, we can write KCLs and KVLs for the MLC circuit in Fig. 3(a) as follows

$$i_{L,k} = i_{M,k} + i_{C,k} \tag{34}$$
$$i_{L,k} = i_{R,k} \tag{35}$$
$$v_{C,k} + v_{R,k} + v_{L,k} - \mu v_{C,k} = 0 \tag{36}$$
$$v_{C,k} = v_{M,k}. \tag{37}$$

Substituting (1) and the first equation of (6) in (34) we obtain

$$i_{L,k} = C\frac{v_{C,k+1} - v_{C,k}}{h} + \frac{\hat{q}(\varphi_{M,k+1}) - \hat{q}(\varphi_{M,k})}{h} \tag{38}$$

while using (3) and (35), from (36) we have

$$(1-\mu)v_{C,k} + Ri_{L,k} + L\frac{i_{L,k+1} - i_{L,k}}{h} = 0. \tag{39}$$

Using (37) we can write the second equation of (6) as

$$\varphi_{M,k+1} = \varphi_{M,k} + hv_{C,k}. \tag{40}$$

Now, (38)-(40) can be straightforwardly recast into (32).

2) Solving (40) with respect to $v_{C,k}$ and substituting in (39) we obtain the following expression

$$i_{L,k} = (\mu - 1)\frac{\varphi_{M,k+1} - \varphi_{M,k}}{Rh} - L\frac{i_{L,k+1} - i_{L,k}}{Rh}.$$

By using (38) and reordering terms we arrive at

$$Cv_{C,k+1} + \frac{Li_{L,k+1}}{R} + \hat{q}(\varphi_{M,k+1}) + \frac{1-\mu}{R}\varphi_{M,k+1} = Cv_{C,k} + \frac{Li_{L,k}}{R} + \hat{q}(\varphi_{M,k}) + \frac{1-\mu}{R}\varphi_{M,k}. \tag{41}$$

3) From (41) we have that, for any $k > 1$,

$$Cv_{C,k} + \frac{Li_{L,k}}{R} + \hat{q}(\varphi_{M,k}) + \frac{1-\mu}{R}\varphi_{M,k} = Q_0$$

i.e., the state variables are bound to evolve on the manifold $\mathcal{M}_{\mathrm{MLC}}(Q_0)$. To derive the equations describing the dynamics on such a manifold, let us write the KqL and KφL for the MLC circuit in Fig. 3(b)

$$q^0_{L,k} = q^0_{M,k} + q^0_{C,k}, \tag{42}$$
$$\varphi^0_{C,k} + \varphi^0_{R,k} + \varphi^0_{L,k} - \mu\varphi^0_{C,k} = 0 \tag{43}$$
$$\varphi^0_{C,k} = \varphi^0_{M,k}. \tag{44}$$

Substituting (2) and (7) in (42) and (4) in (43), and taking into account (44) we have

$$\varphi^0_{M,k+1} = \varphi^0_{M,k} - \frac{h}{C}\hat{q}(\varphi^0_{M,k} + \varphi_{M,0}) + \frac{h}{C} q^0_{L,k} + h v_{C,0} + \frac{h}{C}\hat{q}(\varphi_{M,0})$$

$$q^0_{L,k+1} = \left(1 - \frac{hR}{L}\right) q^0_{L,k} + h i_{L,0} + \frac{h}{L}(\mu - 1)\varphi^0_{M,k}$$

which can be recast into (33) by summing $\varphi_{M,0}$ to both sides of the first equation and taking into account the expressions of y_k and Q_0. ■

Finally, let us consider the dual of the circuit in Fig. 3, i.e., DMLC, which is depicted in Fig. 4(a) (VCD). The corresponding circuit in the FCD is shown in Fig. 4(b).

Proposition 4: The following results hold:

1) In the VCD the dynamics of DMLC is described by the three-dimensional map in the state variables $i_{L,k}, v_{C,k}$ and $q_{M,k}$

$$\begin{cases} i_{L,k+1} = i_{L,k} - \dfrac{\hat{\varphi}(q_{M,k} + h i_{L,k}) - \hat{\varphi}(q_{M,k})}{L} + \dfrac{h}{L} v_{C,k} \\ v_{C,k+1} = (1 - \dfrac{h}{RC}) v_{C,k} + \dfrac{h}{C}(\nu - 1) i_{L,k} \\ q_{M,k+1} = q_{M,k} + h i_{L,k}. \end{cases} \tag{45}$$

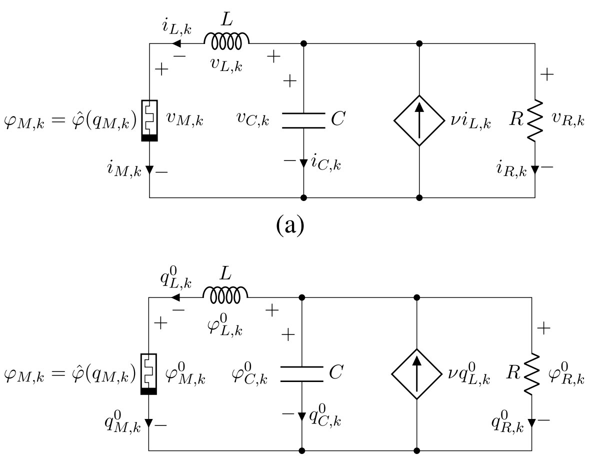

FIGURE 4. DT DMLC circuit. (a) VCD and (b) FCD.

2) The function of the state variables given by

$$\Theta_{\mathrm{DMLC}}(v_C, i_L, q_M) = RCv_C + Li_L + \hat{\varphi}(q_M) + R(1-\nu)q_M$$

is a first integral of (32) for any step size h, i.e., we have $\Theta_{\mathrm{DMLC}}(v_{C,k+1}, i_{L,k+1}, q_{M,k+1}) = \Theta_{\mathrm{DMLC}}(v_{C,k}, i_{L,k}, q_{M,k})$, $k = 0, 1, 2, \ldots$.

3) The state space of (32) is foliated in two-dimensional invariant manifolds

$$\begin{aligned}\mathcal{M}_{\mathrm{DMLC}}(\Phi_0) = \{(v_C, i_L, q_M) \in \mathbb{R}^3 : \Theta_{\mathrm{DMLC}}(v_C, i_L, q_M) &= CRv_C + Li_L + \hat{\varphi}(q_M) + R(1-\nu)q_M \\ &= \Phi_0\}\end{aligned}$$

where $\Phi_0 \in \mathbb{R}$ is the manifold index. On each manifold, i.e., in the FCD, the dynamics is described by the two-dimensional map in the state variables $q_{M,k}$ and $y_k = \varphi^0_{C,k} + R(\nu - 1)q_{M,0} - CRv_{C,0}$

$$\begin{cases} q_{M,k+1} = q_{M,k} + \dfrac{h}{L} y_k - \dfrac{h}{L}\hat{\varphi}(q_{M,k}) + \dfrac{h}{L}\Phi_0 \\ y_{k+1} = (1 - \dfrac{h}{RC}) y_k + \dfrac{h}{C}(\nu - 1) q_{M,k}. \end{cases} \tag{46}$$

■

Proof: 1) First, write KCLs and KVLs for the DMLC circuit in Fig. 4(a) as follows

$$v_{C,k} = v_{L,k} + v_{M,k} \tag{47}$$

$$v_{C,k} = v_{R,k} \tag{48}$$

$$i_{L,k} + i_{R,k} + i_{C,k} - \nu i_{L,k} = 0 \tag{49}$$

$$i_{L,k} = i_{M,k}. \tag{50}$$

Substituting (3) and the first equation (9) in (47) we obtain

$$v_{C_k} = L\frac{i_{L,k+1} - i_{L,k}}{h} + \frac{\hat{\varphi}(q_{M,k+1}) - \hat{\varphi}(q_{M,k})}{h} \tag{51}$$

while using (1) and (48), from (49) we obtain

$$(1-\nu) i_{L,k} + C\frac{v_{C,k+1} - v_{C,k}}{h} + \frac{v_{C,k}}{R} = 0. \tag{52}$$

Exploiting (50) we can write the second equation of (9) as

$$q_{M,k+1} = q_{M,k} + h i_{L,k}. \tag{53}$$

Now, (51)-(53) can be straightforwardly recast into (45).

2) Solving (53) with respect to $i_{L,k}$ and substituting in (52) we obtain the following expression

$$v_{C,k} = R(\nu - 1)\frac{q_{M,k+1} - q_{M,k}}{h} - RC\frac{v_{C,k+1} - v_{C,k+1}}{h}.$$

Equating the right hand sides of the latter equation and (51) and reordering the terms we have

$$\begin{aligned} &RCv_{C,k+1} + Li_{L,k+1} + \hat{\varphi}(q_{M,k+1}) + R(1-\nu)q_{M,k+1} \\ &\quad = RCv_{C,k} + Li_{L,k} + \hat{\varphi}(q_{M,k}) + R(1-\nu)q_{M,k}. \end{aligned} \tag{54}$$

3) Using (54) we have that, for any $k > 1$,

$$RCv_{C,k} + Li_{L,k} + \hat{\varphi}(q_{M,k}) + R(1-\nu)q_{M,k} = \Phi_0$$

i.e., the state variables are bound to evolve on the manifold $\mathcal{M}_{\mathrm{DMLC}}(\Phi_0)$. To write the dynamics on such a manifold, let us write the KqL and KφL for the DMLC circuit in Fig. 4(b)

$$\varphi^0_{C,k} = \varphi^0_{M,k} + \varphi^0_{L,k} \tag{55}$$

$$q^0_{C,k} + q^0_{L,k} + q^0_{R,k} - \nu q^0_{L,k} = 0 \tag{56}$$

$$q^0_{L,k} = q^0_{M,k}. \tag{57}$$

Substituting (4) and (10) in (55) and (2) in (56), and taking into account (57) we obtain

$$q^0_{M,k+1} = q^0_{M,k} - \frac{h}{L}\hat{\varphi}(q^0_{M,k} + q_{M,0}) + \frac{h}{L}\varphi^0_{L,k} + h i_{L,0} + \frac{h}{L}\hat{\varphi}(q_{M,0})$$

$$\varphi^0_{C,k+1} = \left(1 - \frac{h}{RC}\right)\varphi^0_{C,k} + h v_{C,0} + \frac{h}{C}(\nu - 1) q^0_{M,k}.$$

This can be recast as (46) by summing $q_{M,0}$ to both sides of the first equation, and taking into account the expressions of y_k and Φ_0. ■

For the MLC, let $x_k = \varphi_{M,k}$, $z_k = i_{L,k}$, $w_k = v_{C,k}$, $F(\cdot) = \hat{q}(\cdot)$, $\delta = 1/C$, $\beta = R/L$, $\gamma = (\mu - 1)/L$, while for DMLC, let $x_k = q_{M,k}$, $z_k = v_{C,k}$, $w_k = i_{L,k}$, $F(\cdot) = \hat{\varphi}(\cdot)$, $\delta = 1/L$, $\beta = 1/(CR)$, $\gamma = (\nu - 1)/C$. Then, the dynamics in the VCD of both circuits obeys the three-dimensional map in the state variables w_k, z_k and x_k

$$\begin{cases} w_{k+1} = w_k - \delta(F(x_k + hw_k) - F(x_k)) + \delta h z_k \\ z_{k+1} = (1 - h\beta)z_k + h\gamma w_k \\ x_{k+1} = x_k + hw_k. \end{cases} \tag{58}$$

There is a first integral given by

$$\Theta(x, w, z) = \frac{1}{\delta}w + \frac{1}{\beta}z - \frac{\gamma}{\beta}x + F(x) \tag{59}$$

and the state space in the VCD is foliated in the invariant manifolds

$$\mathcal{M}(I_0) = \{(x, w, z) \in \mathbb{R}^3 : \Theta(x, w, z) = \frac{1}{\delta}w + \frac{1}{\beta}z - \frac{\gamma}{\beta}x + F(x) = I_0\}$$

where $I_0 \in \mathbb{R}$ is the manifold index.

Moreover, let for MLC $y_k = q^0_{L,k} - \frac{z_0}{\beta} + \frac{\gamma}{\beta}x_0$ and $I_0 = Q_0$, while for DMLC, let $y_k = \varphi^0_{C,k} - \frac{z_0}{\beta} + \frac{\gamma}{\beta}x_0$ and $I_0 = \Phi_0$. Then, on each invariant manifold the dynamics in the FCD of both circuits is described by the two-dimensional map in the state variables x_k and y_k

$$\begin{cases} x_{k+1} = x_k + h\delta y_k - h\delta F(x_k) + h\delta I_0 \\ y_{k+1} = y_k - h\beta y_k + h\gamma x_k. \end{cases} \tag{60}$$

III. EMBEDDING THE LOGISTIC AND TENT MAP IN THE MC AND ML CIRCUIT

We have seen in Sect. II-B that on each given invariant manifold the dynamics of an MC or an ML circuit obeys a one-dimensional map which depends upon the circuit parameters R and C or R and L, the memristor nonlinearity $\hat{q}$ or $\hat{\varphi}$, the discretization step h and the index I_0 of the invariant manifold. Moreover, in Sect. II-C we have shown along similar lines that the dynamics on each invariant manifold of an MLC circuit and its dual obeys a two-dimensional map depending once more on circuit parameters, discretization step, memristor nonlinearity and invariant manifold index. In Sect. III-A, we address a fundamental design problem, i.e., to select, if it is possible, the circuit parameters, nonlinearity, discretization step and manifold index of an MC and ML circuit so that the map on each manifold coincides with a logistic or a tent map. An analogous design problem is addressed in Sect. IV, i.e., to implement the Hénon or the Lozi map on each invariant manifold of an MLC circuit or its dual.

A. LOGISTIC MAP

The logistic map became popular due to a paper published in Nature in 1976 by biologist Robert May and entitled ‘Simple mathematical models with very complicated dynamics’ [68]. The logistic map is an equation for population growth

$$P_{k+1} = rP_k(1 - P_k) \tag{61}$$

where the next generation population P_{k+1} is determined by the population P_k in the current generation, the rate r at which individuals reproduce and the level of available resources given that the system has a finite capacity. According to May, such a one-dimensional map, ‘even though simple and deterministic, can exhibit a surprising array of dynamical behaviour, from stable points, to a bifurcating hierarchy of stable cycles, to apparently random fluctuations’ [68].

Consider the change of variables $x_k = rP_k - r/2$. This yields from (61) the map

$$x_{k+1} = -x_k^2 + a \tag{62}$$

where $a = -r/2 + r^2/4 \in \mathbb{R}$ is a scalar parameter. The maps (61) and (62) are topologically conjugate [56].

Let us now address the main design problem considered in the paper, i.e., to determine, if it possible, the circuit parameters, memristor nonlinearity, discretization step and manifold index of an MC or ML circuit so that the one-dimensional map on each manifold coincides with the logistic map. To this end, let us compare (62) with (31). On this basis it is seen that the dynamics of an MC or an ML circuit in the FCD is exactly described by the logistic map (62), provided we choose $h\delta I_0 = a$ and $F(x) = (x + x^2)/(h\delta)$. One possible solution to these constraints is given by

$$h = 1, \quad \delta = 1, \quad F(x) = x^2 + x, \quad I_0 = a. \tag{63}$$

Summing up, under the conditions (63), the dynamics in the VCD of an MC or an ML circuit obeys the two-dimensional map (cf. (29))

$$\begin{cases} y_{k+1} = y_k - (F(x_k + y_k) - F(x_k)) = -y_k^2 - 2x_k y_k \\ x_{k+1} = x_k + y_k. \end{cases} \tag{64}$$

The map (64) has the first integral (cf. (30))

$$\Theta(x, y) = y + x + x^2$$

and the two-dimensional state space (x, y) is foliated in one-dimensional invariant manifolds

$$\mathcal{M}(a) = \{(x, y) \in \mathbb{R}^2 : \Theta(x, y) = y + x + x^2 = a\} \tag{65}$$

where $a \in \mathbb{R}$ is the manifold index. On each manifold the dynamics is described in the FCD by the logistic map

$$x_{k+1} = -x_k^2 + a. \tag{66}$$

Next, we show that the two-dimensional map (64) in the VCD displays an extremely rich dynamics due to the foliation of its state space and the property of extreme multistability.

Moreover, we provide simulations to illustrate and verify the predicted behavior.

We have seen that on an invariant manifold with index a the two-dimensional map (64) embeds the logistic map (66) with parameter a. First, for convenience of exposition, let us briefly recall some basic facts about the logistic map, see for instance [55]. The classic bifurcation diagram of the logistic map is shown in Fig. 5, where we considered for simplicity the case $a \geq 0$. When $0 \leq a \leq 2$ the orbits are bounded, while when $a > 2$ orbits escape to infinity. The orbits approach a stable fixed point when $0 \leq a \leq a_1 = 3/4$. At $a_1 = 3/4$, a flip (or period-doubling) bifurcation occurs with the birth of a stable period-two cycle. By increasing a, we observe a second flip bifurcation at $a_2 = 5/4$ where the period-two cycle gives birth to a stable period-four cycle. This is followed by a typical cascade of period-doubling bifurcations accumulating at $a_\infty = 1.401\ldots$. These bifurcations originate the birth of a complex attractor for $a > a_\infty$.

Let us now come back to the two-dimensional map (64) in the VCD and verify via simulations with MATLAB the correctness of the predicted dynamical behavior. Its invariant manifolds (cf. 65)

$$y = a - x^2 - x$$

for some relevant values of a are depicted in Fig. 6. Note that they have a reverse U-shape due to the quadratic term $-x^2$. The same figure shows for each manifold the transient part (green dots) and the attractor (red dots) of an orbit starting on the manifold and evolving, due to its invariance, on the same manifold. When $a = 0.5$ we have convergence to a fixed point, while when $a_1 < a = 1 < a_2$ there is convergence to a period-two cycle and when $a = 1.3 > a_2$ we observe convergence to a period-four cycle. Moreover, when $a = 1.627$ the orbit converges to a period-five cycle while when $a = 1.95$ we observe convergence to a complex attractor. The corresponding time-domain evolution of orbits for large k is shown in Fig. 7. Fig. 8 displays the bifurcation diagram of x and y when varying the manifold index a. Note that the bifurcation diagram of x coincides with that of the logistic map shown in Fig. 5, confirming that the two-dimensional map (64) embeds as predicted the logistic map (62). A three-dimensional view of the bifurcation diagram of the map (64) in the space (x, y, a) is in Fig 9.

Remark 2: It is important to stress that, *given any parameter $a \in \mathbb{R}$, the dynamics of the logistic map (62) with parameter a is embedded in the invariant manifold with index a of the two-dimensional map (64). Therefore, all the different dynamics and attractors of the logistic map are embedded as a whole in the set of invariant manifolds of the map (64).* This very rich behavior with infinitely many coexisting attractors is an instance of the property of extreme multistability enjoyed by maps of DT memristor circuits [69]. ■

Remark 3: Consider again the two-dimensional map (64). It can be verified that the map has a line of fixed points given by $(\bar{y}, \bar{x}) = (0, \chi)$, where χ is any value in $\mathbb{R}$. The previous results can also be interpreted this way. Suppose that by changing the index a of the manifold we move along the line of fixed points. When $0 \leq a \leq a_1$ the positive fixed point is stable. At $a = a_1$ the fixed point loses stability via a flip bifurcation. We note that this bifurcation happens for fixed parameters in the map (64), hence we are dealing with a so-called flip-bifurcation without parameters [63]. Similarly, we observe a second flip bifurcation without parameters at $a = a_2$ and a subsequent cascade of flip bifurcations without parameters for $a > a_2$. ■

Remark 4: It is possible to embed also other classic one-dimensional maps into the two-dimensional map (64). Consider for example the tent map [55]

$$x_{k+1} = \begin{cases} ax, & x < 0.5 \\ a(1-x), & x \geq 0.5 \end{cases} \tag{67}$$

where $a \in \mathbb{R}$ is a parameter. This can be transformed into the logistic map (61) via the homeomorphism [56]

$$h(x) = \frac{2}{\pi} \arcsin(\sqrt{x})$$

and hence the two maps are topologically conjugate. Thereafter, we can proceed by the devised technique to embed the tent map into the MC or the ML circuit (we omit the details). ■

Remark 5: There are intervals of parameters a where chaos in the sense of Devaney and Li-Yorke can be rigorously proved for the logistic map (62) [55]. Since the DT MC and ML circuits exactly embed on the invariant manifolds the logistic map, it follows that we have constructed a class of memristor circuits where chaos can be analytically proved. This differs from results in the literature where chaos in DT memristor circuits is studied via numerical means as simulations, bifurcation diagrams and Lyapunov exponents. ■

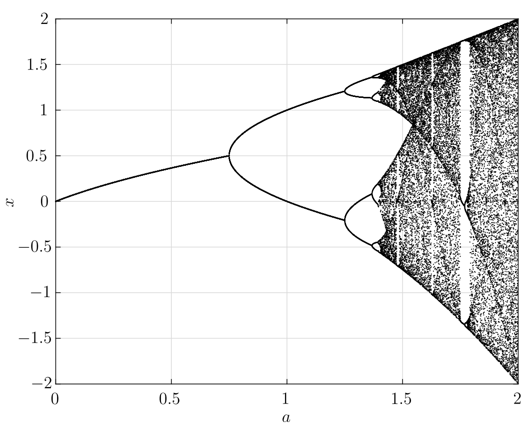

FIGURE 5. Bifurcation diagram of the logistic map (62) obtained by varying parameter *a*.

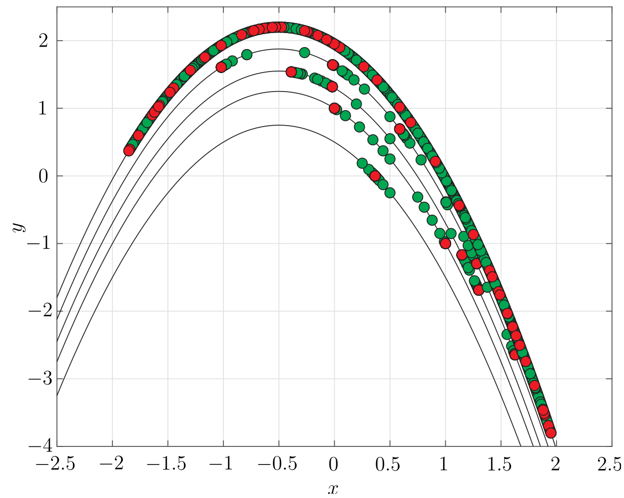

FIGURE 6. Curves from bottom to top: (reverse) U-shaped invariant manifolds $\mathcal{M}(a)$ of the two-dimensional map (64), see (65), when $a \in \{0.5, 1, 1.3, 1.627, 1.95\}$. On each manifold the figure shows the evolution of an orbit of (64) starting on $\mathcal{M}(a)$ (green circles), as well as the long-term behavior of each orbit (red circles), as obtained with MATLAB simulations.

IV. EMBEDDING THE HÉNON AND LOZI MAP IN THE MLC AND DMLC CIRCUIT

The celebrated Lorenz system is a three-dimensional system of ordinary differential equations modeling the convection and temperature variation of a hydrodynamical system. The system, presented by Edward Lorenz in a 1963 paper entitled 'Deterministic Nonperiodic Flow' [70], for suitable parameter values has a complex attractor and from simulations almost all its orbits appear to be of a nonperiodic nature. Later on, in the 1976 article entitled 'A Two-dimensional Mapping with a Strange Attractor', Michel Hénon introduced a two-dimensional map constructed as a simplified model of the Poincare's section of the Lorenz system [71] that inherits the stretch and folding mechanism leading to chaos in Lorenz system. The Hénon map actually provides a more tractable mathematical model useful for better understanding Lorenz system. Hénon map has been deeply studied and it is still the subject of intense investigation.

The two-dimensional Hénon map is given as

$$\begin{cases} X_{k+1} = 1 - aX_k^2 + Y_k \\ Y_{k+1} = bX_k \end{cases} \tag{68}$$

where $a, b \in \mathbb{R}$ are two parameters. For suitable parameters the map can display a chaotic attractor while for other parameter values it shows a convergent or a periodic behavior.

Let us consider the change of variables $x_k = aX_k$ and $y_k = aY_k$. We obtain from (68) the two-dimensional map

$$\begin{cases} x_{k+1} = -x_k^2 + y_k + a \\ y_{k+1} = bx_k. \end{cases} \tag{69}$$

The two maps (68) and (69) are topologically conjugate. As an example, Fig. 10 shows the chaotic attractor with a boomerang-like shape of Hénon map (69) obtained for the

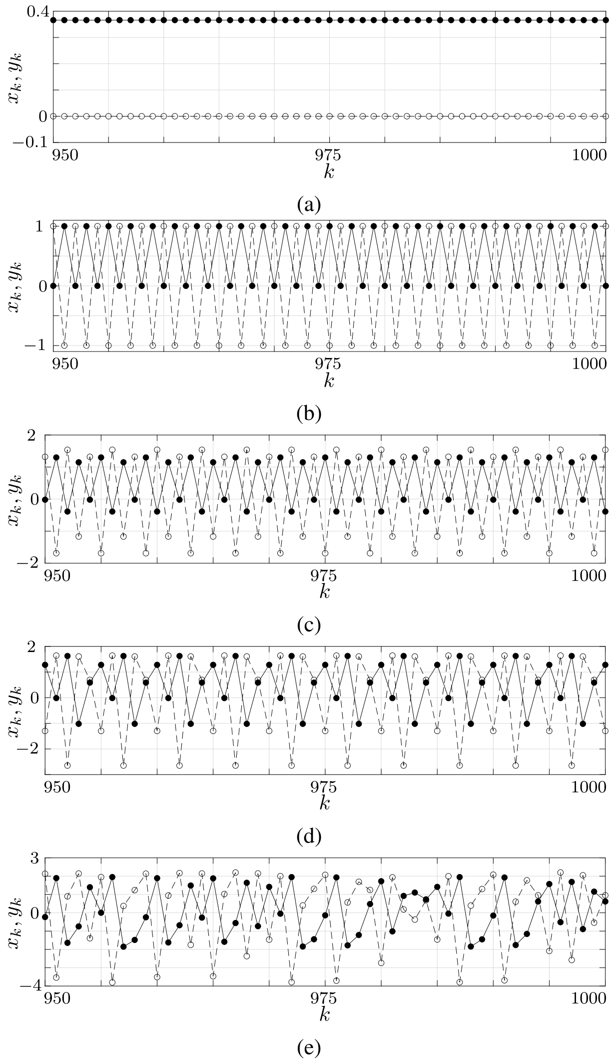

FIGURE 7. Long-term behavior of the orbits of the two-dimensional map (64) for different values of the manifold index a. For better visualization, the values x_k (resp., y_k) are connected by solid (resp., dashed) lines. (a) Fixed point for $a = 0.5$, (b) period-two cycle for $a = 1$, (c) period-four cycle for $a = 1.3$, (d) period-five cycle when $a = 1.627$, (e) complex attractors when $a = 1.95$.

traditional parameters $a = 1.4$ and $b = 0.3$ considered in [71], while Fig. 11 shows the bifurcation diagram of x when parameter a is varied and $b = 0.3$.

Let us now address the main design problem considered in the paper, i.e., to determine, if it possible, the circuit parameters, memristor nonlinearity, discretization step and manifold index of an MLC circuit or its dual so that the map on each manifold coincides with the Hénon map. Comparing (60) with (69), it is easy to see that the dynamics of an MLC or a DMLC circuit is exactly described in the FCD by the Hénon map (69), provided we choose $h\delta = 1$, $h\beta = 1$, $h\gamma = b$, $F(x) = x + x^2$ and $I_0 = a$. One possible solution is given by

$$h = 1, \quad \delta = \beta = 1, \quad \gamma = b, \quad F(x) = x^2 + x, \quad I_0 = a. \tag{70}$$

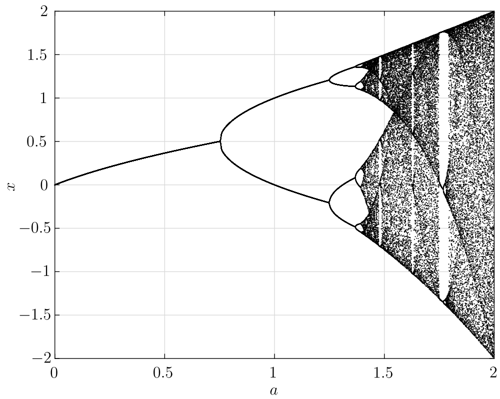

(a)

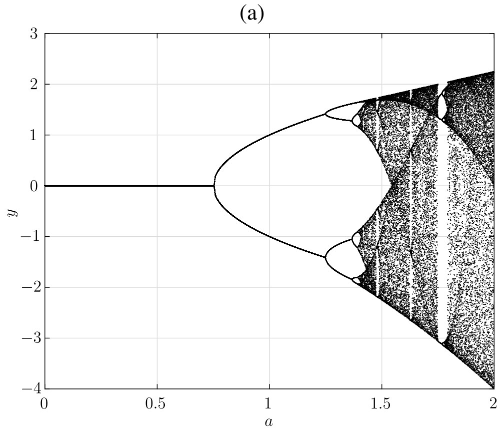

(b)

FIGURE 8. a) Bifurcation diagrams of the two-dimensional map (64) obtained by varying parameter a: a) variable x and b) variable y.

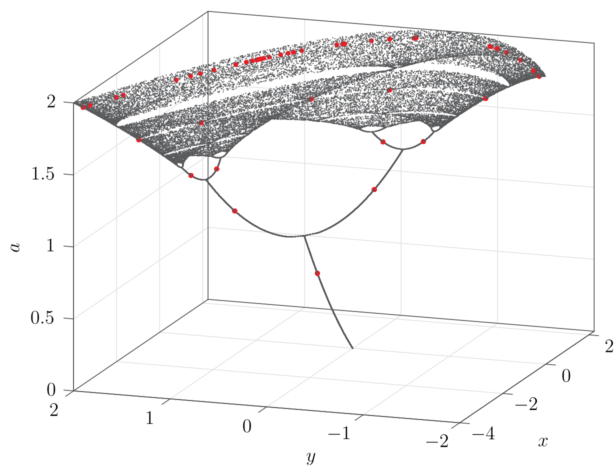

FIGURE 9. A three-dimensional view of the bifurcation diagram of the two-dimensional map (64) in the space (x, y, a) obtained by varying parameter a.

We can wrap up these results as follows. Under the conditions (70), the dynamics in the VCD of an MLC or a DMLC circuit obeys the three-dimensional map (cf. (58))

$$\begin{cases} w_{k+1} = w_k - (F(x_k + w_k) - F(x_k)) + z_k \\ = -w_k^2 - 2x_k w_k + z_k \\ z_{k+1} = bw_k \\ x_{k+1} = x_k + w_k. \end{cases} \tag{71}$$

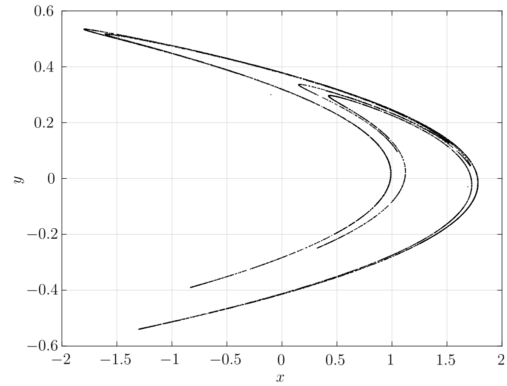

FIGURE 10. Attractor displayed by Hénon map (69) when $a = 1.4$ and $b = 0.3$..

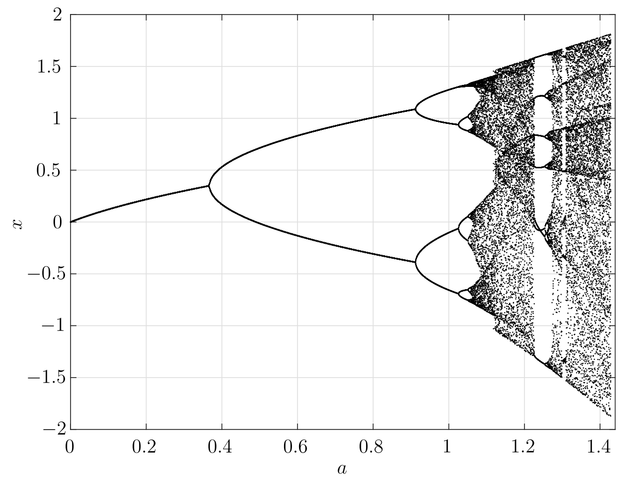

FIGURE 11. Bifurcation diagram of variable x for the Hénon map (69) obtained by varying parameter a when $b = 0.3$.

The map (71) has the first integral (cf. (59))

$$\Theta(x, w, z) = w + z - bx + x + x^2$$

and the three-dimensional state space (x, w, z) is foliated in one-dimensional invariant manifolds

$$\mathcal{M}(a) = \{(x, w, z) \in \mathbb{R}^3 : \Theta(x, w, z) = w + z \tag{72}$$
$$- bx + x + x^2 = a\} \tag{73}$$

where $a \in \mathbb{R}$ is the manifold index. It turns out that on each manifold the dynamics is described in the FCD by the Hénon map (cf. 60)

$$\begin{cases} x_{k+1} = -x_k^2 + y_k + a \\ y_{k+1} = bx_k. \end{cases} \tag{74}$$

The three-dimensional map (71) in the VCD displays an extremely rich dynamics due to the foliation of its state space and the property of extreme multistability. Fig. 12 shows the bifurcation diagram of variables x of (71) obtained by varying a when $b = 0.3$, as obtained with MATLAB simulations. This coincides with that in Fig. 11, confirming that (71) embeds the Hénon map for the considered parameters and memristor nonlinearity.

Remark 6: Once more we stress that, *given any parameter $a \in \mathbb{R}$, the dynamics of the Hénon map (69) with parameter a is embedded in the invariant manifold with index a of the three-dimensional map (71). Therefore, all the different dynamics and attractors of the Hénon map are embedded as a whole in the set of invariant manifolds of the map (71).* This extremely rich behavior with infinitely many coexisting attractors is once more a consequence of the property of extreme multistability of DT maps implemented by memristor circuits [69]. ■

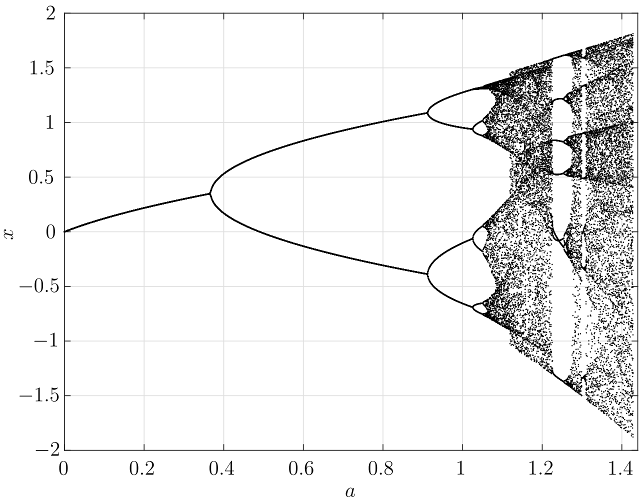

FIGURE 12. **Bifurcation diagram of variable x three-dimensional map (71) obtained by varying parameter a when $b = 0.3$.**

Remark 7: If we eliminate the controlled sources in the MLC or DMLC, i.e., we put $\mu = 0$ or $\nu = 0$, respectively, it is seen that the simplified MLC and DMLC circuits can implement a variant of Hénon map where parameter $b < 0$. Such a variant is still able to display interesting complex behaviors as discussed for instance in [64]. ■

Remark 8: In 1978, in a short note entitled 'Un attracteur étrange (?) du type attracteur de Hénon' [72], René Lozi proposed [1] the following two-dimensional map

$$\begin{cases} x_{k+1} = 1 - a|x_k| + y_k \\ y_{k+1} = bx_k \end{cases} \tag{75}$$

where $a, b \in \mathbb{R}$ are two parameters. The defining equations are exactly those of the Hénon map, provided a quadratic term in Hénon map is replaced with a piecewise linear term in Lozi map. This permits to rigorously prove the chaotic character of some attractors and to arrive at a detailed analysis of attraction basins. In his original paper, Lozi used the parameters $a = 1.7$ and $b = 0.5$ to obtain a complex attractor with an edgy boomerang-like shape whose chaotic nature was rigorously proved by Michal Misiurewicz [73]. A review on Lozi maps and its applications is provided in [74], [75]. Again, it is not difficult to show that we can embed Lozi map in an MLC circuit or its dual by appropriately choosing the parameters and the piecewise linear memristor nonlinearity (details are left to the interested reader). ■

V. CONCLUSION

One relevant fact that emerges in the literature is that maps obtained by discretizing simple memristor circuits are able to display via simulations an unexpectedly rich dynamic behavior including chaos and hyperchaos. This paper has provided a rationale to explain this complex dynamics via the analysis of two simple classes of DT memristor circuits obtained via DT-FCAM. Firstly, a DT circuit composed of a capacitor plus a flux-controlled memristor and its dual, have been considered. It is shown that the two-dimensional map in the VCD of the circuits can exactly embed on the invariant manifolds, i.e., in the FCD, two classic chaotic one-dimensional maps, i.e., the logistic and the tent map. Secondly, a DT memristor Murali-Lakshmanan-Chua and its dual, have been considered. The paper has shown that the three-dimensional map in the VCD of the circuits can exactly embed on the invariant manifolds two classic chaotic two-dimensional maps, i.e., the Hénon and the Lozi map. One significant result is that we can exploit the property of extreme multistability of the DT memristor circuits to simultaneously embed in the set of invariant manifolds all possible dynamics obtained by varying one parameter in the logistic or in the Hénon map. The main conclusion is that observing complex dynamics even in maps obtained by discretizing the simplest memristor circuits is not surprising at all.

REFERENCES

[1] L. Chua, "Memristor—The missing circuit element," *IEEE Trans. Circuit Theory*, vol. CT-18, no. 5, pp. 507–519, Jun. 1971.
[2] D. B. Strukov, G. S. Snider, D. R. Stewart, and R. S. Williams, "The missing memristor found," *Nature*, vol. 453, no. 7191, pp. 80–83, May 2008.
[3] P. Mazumder, S. M. Kang, and R. Waser, "Special issue on memristors: Devices, models, and applications," *Proc. IEEE*, vol. 100, no. 6, Jun. 2012.
[4] L. Chua, G. Sirakoulis, and A. Adamatzky, *Handbook of Memristor Networks*, vol. 1, 2nd ed., New York, NY, USA: Springer, 2019.
[5] R. Tetzlaff, *Memristors and Memristive Systems*. New York, NY, USA: Springer, 2014.
[6] F. Corinto, M. Forti, and L. O. Chua, *Nonlinear Circuits and Systems With Memristors*. Cham, Switzerland: Springer, 2021.
[7] T. Huang, Y. Chen, Z. Zeng, and L. Chua, "Editorial special issue for 50th birthday of memristor theory and application of neuromorphic computing based on memristor—Part I," *IEEE Trans. Circuits Syst. I, Reg. Papers*, vol. 68, no. 11, pp. 4417–4418, Nov. 2021.
[8] K. Datta and R. Drechsler, "Special issue on in-memory computing: Circuits, system, architecture and verification," *Memories-Mater., Devices, Circuits Syst.*, vol. 5, Oct. 2023, Art. no. 100062.
[9] J. J. Yang and R. S. Williams, "Memristive devices in computing system: Promises and challenges," *ACM J. Emerg. Technol. Comput. Syst.*, vol. 9, no. 2, p. 11, May 2013.
[10] A. Sebastian, M. Le Gallo, G. W. Burr, S. Kim, M. BrightSky, and E. Eleftheriou, "Tutorial: Brain-inspired computing using phase-change memory devices," *J. Appl. Phys.*, vol. 124, no. 11, Sep. 2018, Art. no. 111101.
[11] A. P. James, K. N. Salama, H. Li, D. Biolek, G. Indiveri, and L. O. Chua, "Guest editorial: Special issue on large-scale memristive systems and neurochips for computational intelligence," *IEEE Trans. Emerg. Topics Comput. Intell.*, vol. 2, no. 5, pp. 320–323, Oct. 2018.
[12] G. Ch. Sirakoulis, A. Ascoli, R. Tetzlaff, and S. Yu, "Guest editorial memristive circuits and systems for edge-computing applications," *IEEE J. Emerg. Sel. Topics Circuits Syst.*, vol. 12, no. 4, pp. 717–722, Dec. 2022.
[13] F. Zahoor, T. Z. Azni Zulkifli, and F. A. Khanday, "Resistive random access memory (RRAM): An overview of materials, switching mechanism, performance, multilevel cell (MLC) storage, modeling, and applications," *Nanosc. Res. Lett.*, vol. 15, no. 1, Dec. 2020.

[14] S. S. Sarwar, S. A. N. Saqueb, F. Quaiyum, and A. B. M. H. Rashid, ''Memristor-based nonvolatile random access memory: Hybrid architecture for low power compact memory design,'' *IEEE Access*, vol. 1, pp. 29–34, 2013.
[15] B. Hajri, H. Aziza, M. M. Mansour, and A. Chehab, ''RRAM device models: A comparative analysis with experimental validation,'' *IEEE Access*, vol. 7, pp. 168963–168980, 2019.
[16] R. S. Williams, ''What's next? [The end of Moore's law],'' *Comput. Sci. Eng.*, vol. 19, no. 2, pp. 7–13, Mar. 2017.
[17] M. A. Zidan, J. P. Strachan, and W. D. Lu, ''The future of electronics based on memristive systems,'' *Nature Electron.*, vol. 1, no. 1, pp. 22–29, Jan. 2018.
[18] D. Ielmini and G. Pedretti, ''Device and circuit architectures for in-memory computing,'' *Adv. Intell. Syst.*, vol. 2, no. 7, Jul. 2020, Art. no. 2000040.
[19] A. Ascoli, A. S. Demirkol, R. Tetzlaff, and L. Chua, ''Edge of chaos theory resolves smale paradox,'' *IEEE Trans. Circuits Syst. I, Reg. Papers*, vol. 69, no. 3, pp. 1252–1265, Mar. 2022.
[20] W. Yan, W. Dong, P. Wang, Y. Wang, Y. Xing, and Q. Ding, ''Discrete-time memristor model for enhancing chaotic complexity and application in secure communication,'' *Entropy*, vol. 24, no. 7, p. 864, Jun. 2022.
[21] S. Kumar, J. P. Strachan, and R. S. Williams, ''Chaotic dynamics in nanoscale NbO_2 Mott memristors for analogue computing,'' *Nature*, vol. 548, no. 7667, pp. 318–321, Aug. 2017.
[22] Y. Liang, G. Wang, G. Chen, Y. Dong, D. Yu, and H. H. Iu, ''S-type locally active memristor-based periodic and chaotic oscillators,'' *IEEE Trans. Circuits Syst. I, Reg. Papers*, vol. 67, no. 12, pp. 5139–5152, Dec. 2020.
[23] S. He, K. Sun, Y. Peng, and L. Wang, ''Modeling of discrete fracmemristor and its application,'' *AIP Adv.*, vol. 10, no. 1, Jan. 2020.
[24] B. Bao, H. Li, H. Wu, X. Zhang, and M. Chen, ''Hyperchaos in a second-order discrete memristor-based map model,'' *Electron. Lett.*, vol. 56, no. 15, pp. 769–770, Jul. 2020.
[25] Y. Peng, S. He, and K. Sun, ''A higher dimensional chaotic map with discrete memristor,'' *AEU-Int. J. Electron. Commun.*, vol. 129, Feb. 2021, Art. no. 153539.
[26] M. Ma, Y. Yang, Z. Qiu, Y. Peng, Y. Sun, Z. Li, and M. Wang, ''A locally active discrete memristor model and its application in a hyperchaotic map,'' *Nonlinear Dyn.*, vol. 107, no. 3, pp. 2935–2949, Feb. 2022.
[27] Q. Lai, L. Yang, and G. Chen, ''Design and performance analysis of discrete memristive hyperchaotic systems with stuffed cube attractors and ultraboosting behaviors,'' *IEEE Trans. Ind. Electron.*, vol. 71, no. 7, pp. 7819–7828, Jul. 2024.
[28] H. Bao, H. Li, Z. Hua, Q. Xu, and B. Bao, ''Sine-transform-based memristive hyperchaotic model with hardware implementation,'' *IEEE Trans. Ind. Informat.*, vol. 19, no. 3, pp. 2792–2801, Mar. 2023.
[29] L. J. Liu, Y. H. Qin, and D. Q. Wei, ''Dynamics of discrete memristor-based Rulkov neuron,'' *IEEE Access*, vol. 10, pp. 72051–72056, 2022.
[30] Y. Peng, K. Sun, and S. He, ''A discrete memristor model and its application in Hénon map,'' *Chaos, Solitons Fractals*, vol. 137, May 2020, Art. no. 109873.
[31] H. Li, Z. Hua, H. Bao, L. Zhu, M. Chen, and B. Bao, ''Two-dimensional memristive hyperchaotic maps and application in secure communication,'' *IEEE Trans. Ind. Electron.*, vol. 68, no. 10, pp. 9931–9940, Oct. 2021.
[32] H. Bao, Z. Hua, H. Li, M. Chen, and B. Bao, ''Discrete memristor hyperchaotic maps,'' *IEEE Trans. Circuits Syst. I, Reg. Papers*, vol. 68, no. 11, pp. 4534–4544, Nov. 2021.
[33] Y. Li, C. Li, Y. Zhao, and S. Liu, ''Memristor-type chaotic mapping,'' *Chaos, Interdiscipl. J. Nonlinear Sci.*, vol. 32, no. 2, Feb. 2022.
[34] Y.-M. Lu, C.-H. Wang, Q.-L. Deng, and C. Xu, ''The dynamics of a memristor-based Rulkov neuron with fractional-order difference,'' *Chin. Phys. B*, vol. 31, no. 6, Jun. 2022, Art. no. 060502.
[35] Y. Deng and Y. Li, ''Nonparametric bifurcation mechanism in 2-D hyperchaotic discrete memristor-based map,'' *Nonlinear Dyn.*, vol. 104, no. 4, pp. 4601–4614, Jun. 2021.
[36] X. Liu, K. Sun, H. Wang, and S. He, ''A class of novel discrete memristive chaotic map,'' *Chaos, Solitons Fractals*, vol. 174, Sep. 2023, Art. no. 113791.
[37] H. Li, C. Li, and J. Du, ''Discretized locally active memristor and application in logarithmic map,'' *Nonlinear Dyn.*, vol. 111, no. 3, pp. 2895–2915, Feb. 2023.
[38] L. Ren, J. Mou, S. Banerjee, and Y. Zhang, ''A hyperchaotic map with a new discrete memristor model: Design, dynamical analysis, implementation and application,'' *Chaos, Solitons Fractals*, vol. 167, Feb. 2023, Art. no. 113024.
[39] X. Liu, J. Mou, Y. Zhang, and Y. Cao, ''A new hyperchaotic map based on discrete memristor and meminductor: Dynamics analysis, encryption application, and DSP implementation,'' *IEEE Trans. Ind. Electron.*, vol. 71, no. 5, pp. 5094–5104, Jun. 2024.
[40] H. Bao, Y. Gu, Q. Xu, X. Zhang, and B. Bao, ''Parallel bi-memristor hyperchaotic map with extreme multistability,'' *Chaos, Solitons Fractals*, vol. 160, Jul. 2022, Art. no. 112273.
[41] Q. Lai, Z. Wan, L. K. Kengne, P. D. Kamdem Kuate, and C. Chen, ''Two-Memristor-Based chaotic system with infinite coexisting attractors,'' *IEEE Trans. Circuits Syst. II, Exp. Briefs*, vol. 68, no. 6, pp. 2197–2201, Jun. 2021.
[42] Q. Lai, C. Lai, H. Zhang, and C. Li, ''Hidden coexisting hyperchaos of new memristive neuron model and its application in image encryption,'' *Chaos, Solitons Fractals*, vol. 158, May 2022, Art. no. 112017.
[43] S. Balatti, S. Ambrogio, R. Carboni, V. Milo, Z. Wang, A. Calderoni, N. Ramaswamy, and D. Ielmini, ''Physical unbiased generation of random numbers with coupled resistive switching devices,'' *IEEE Trans. Electron Devices*, vol. 63, no. 5, pp. 2029–2035, May 2016.
[44] A. Pisarchik, R. Jaimes-Reátegui, C. Rodríguez-Flores, J. García-López, G. Huerta-Cuellar, and F. Martín-Pasquín, ''Secure chaotic communication based on extreme multistability,'' *J. Franklin Inst.*, vol. 358, no. 4, pp. 2561–2575, Mar. 2021.
[45] Y. Deng and Y. Li, ''A 2D hyperchaotic discrete memristive map and application in reservoir computing,'' *IEEE Trans. Circuits Syst. II, Exp. Briefs*, vol. 69, no. 3, pp. 1817–1821, Mar. 2022.
[46] S. Xu, J. Ren, M. Ji'e, S. Duan, and L. Wang, ''Application of reservoir computing based on a 2D hyperchaotic discrete memristive map in efficient temporal signal processing,'' *Int. J. Bifurcation Chaos*, vol. 33, no. 6, May 2023.
[47] H. Lin, C. Wang, L. Cui, Y. Sun, C. Xu, and F. Yu, ''Brain-like initial-boosted hyperchaos and application in biomedical image encryption,'' *IEEE Trans. Ind. Informat.*, vol. 18, no. 12, pp. 8839–8850, Dec. 2022.
[48] S. Zhang, H. Zhang, and C. Wang, ''Dynamical analysis and applications of a novel 2-D hybrid dual-memristor hyperchaotic map with complexity enhancement,'' *Nonlinear Dyn.*, vol. 111, no. 16, pp. 15487–15513, Aug. 2023.
[49] F. Yang, J. Mou, K. Sun, Y. Cao, and J. Jin, ''Color image compression-encryption algorithm based on fractional-order memristor chaotic circuit,'' *IEEE Access*, vol. 7, pp. 58751–58763, 2019.
[50] F. Corinto and M. Forti, ''Memristor circuits: Flux—Charge analysis method,'' *IEEE Trans. Circuits Syst. I: Reg. Papers*, vol. 63, no. 11, pp. 1997–2009, Nov. 2016.
[51] M. Di Marco, M. Forti, L. Pancioni, and A. Tesi, ''New class of discrete-time memristor circuits: First integrals, coexisting attractors and bifurcations without parameters,'' *Int. J. Bifurcation Chaos*, vol. 34, no. 1, Jan. 2024, Art. no. 2450001.
[52] B. Bao, Q. Xu, H. Bao, and M. Chen, ''Extreme multistability in a memristive circuit,'' *Electron. Lett.*, vol. 52, no. 12, pp. 1008–1010, Jun. 2016.
[53] M. Di Marco, M. Forti, L. Pancioni, and A. Tesi, ''Snap-back repellers and chaos in a class of discrete-time memristor circuits,'' *Nonlinear Dyn.*, vol. 112, no. 15, pp. 13519–13537, Aug. 2024.
[54] A. I. Ahamed and M. Lakshmanan, ''Nonsmooth bifurcations, transient hyperchaos and hyperchaotic beats in a memristive Murali–Lakshmanan–Chua circuit,'' *Int. J. Bifurcation Chaos*, vol. 23, no. 6, Jun. 2013, Art. no. 1350098.
[55] M. W. Hirsch, S. Smale, and R. L. Devaney, *Differential Equations, Dynamical Systems, and an Introduction to Chaos*. New York, NY, USA: Academic, 2013.
[56] J. Hale and H. Koçak, *Dynamics and Bifurcations*. New York, NY, USA: Springer-Verlag, 1991.
[57] S. Smale, ''On the differential equations of species in competition,'' *J. Math. Biol.*, vol. 3, no. 1, pp. 5–7, 1976.
[58] M. W. Hirsch, ''Convergent activation dynamics in continuous time networks,'' *Neural Netw.*, vol. 2, no. 5, pp. 331–349, Jan. 1989.
[59] M. W. Hirsch, ''Systems of differential equations that are competitive or cooperative II: Convergence almost everywhere,'' *SIAM J. Math. Anal.*, vol. 16, no. 3, pp. 423–439, May 1985.
[60] G. Innocenti, A. Tesi, M. D. Marco, and M. Forti, ''Embedding the dynamics of forced nonlinear systems in multistable memristor circuits,'' *IEEE J. Emerg. Sel. Topics Circuits Syst.*, vol. 12, no. 4, pp. 735–749, Dec. 2022.
[61] J. Nagumo, S. Arimoto, and S. Yoshizawa, ''An active pulse transmission line simulating Nerve Axon,'' *Proc. IRE*, vol. 50, no. 10, pp. 2061–2070, Oct. 1962.

[62] P. J. Holmes and D. A. Rand, "The bifurcations of Duffing's equation: An application of catastrophe theory," *J. Sound Vibrat.*, vol. 44, no. 2, pp. 237–253, Jan. 1976.
[63] F. Corinto and M. Forti, "Memristor circuits: Bifurcations without parameters," *IEEE Trans. Circuits Syst. I, Reg. Papers*, vol. 64, no. 6, pp. 1540–1551, Jun. 2017.
[64] J. Heagy, "A physical interpretation of the Hénon map," *Physica D, Nonlinear Phenomena*, vol. 57, pp. 436–446, Aug. 1992.
[65] K. Murali, M. Lakshmanan, and L. O. Chua, "The simplest dissipative nonautonomous chaotic circuit," *IEEE Trans. Circuits Syst. I, Fundam. Theory Appl.*, vol. 41, no. 6, pp. 462–463, Jun. 1994.
[66] M. Itoh and L. O. Chua, "Memristor scillators," *Int. J. Bifurcation Chaos*, vol. 18, no. 11, pp. 3183–3206, Nov. 2008.
[67] L. O. Chua and R. N. Madan, "Special section on: Chaotic systems," *Proc. IEEE*, Aug. 1987.
[68] R. M. May, "Simple mathematical models with very complicated dynamics," *Nature*, vol. 261, no. 5560, pp. 459–467, Jun. 1976.
[69] M. Di Marco, G. Innocenti, A. Tesi, and M. Forti, "Circuits with a mem-element: Invariant manifolds control via pulse programmed sources," *Nonlinear Dyn.*, vol. 106, no. 3, pp. 2577–2606, Nov. 2021.
[70] E. N. Lorenz, "Deterministic nonperiodic flow," *J. Atmos. Sci.*, vol. 20, no. 2, pp. 130–141, Mar. 1963.
[71] M. Hénon, "A two-dimensional mapping with a strange attractor," *Commun. Math. Phys.*, vol. 50, no. 1, pp. 69–77, Feb. 1976.
[72] R. Lozi, "Un attracteur étrange (?) du type attracteur de Hénon," *Le J. de Phys. Colloques*, vol. 39, no. C5, pp. C5-9–C5-10, Aug. 1978.
[73] M. Misiurewicz, "Strange attractors for the Lozi mappings," *Ann. New York Acad. Sci.*, vol. 357, no. 1, pp. 348–358, Dec. 1980.
[74] Z. Elhadj, *Lozi Mappings: Theory and Applications*. Boca Raton, FL, USA: CRC Press, 2013.
[75] R. Lozi, "Survey of recent applications of the chaotic Lozi map," *Algorithms*, vol. 16, no. 10, p. 491, Oct. 2023.

MAURO DI MARCO was born in Florence, Italy, in 1970. He received the Laurea degree in electronic engineering from the University of Florence, Florence, and the Ph.D. degree from the University of Bologna, Bologna, Italy, in 1997 and 2001, respectively. From November 1999 to April 2000, he held a position as a Visiting Researcher with LAAS, Toulouse, France. Since 2000, he has been with the University of Siena, Siena, Italy, where he is currently an Associate Professor of circuit theory. He is the co-author of more than 110 international journals and conference papers. His current research interests include analysis and modeling of nonlinear dynamics of complex systems and neural networks, in robust estimation and filtering. From 2007 to 2011, he served as an Associate Editor for IEEE Transactions on Circuits and Systems—I: Regular Papers. Since 2020, he has been serving as an Associate Editor for the *Neural Processing Letters* (Springer).

MAURO FORTI received the Laurea degree in electronics engineering from the University of Florence, Italy, in 1988. From 1991 to 1998, he was an Assistant Professor of applied mathematics and network theory with the Electronic Engineering Department, University of Florence. In 1998, he joined the Department of Information Engineering and Mathematics, University of Siena, Italy, where he is currently a Professor of electrical engineering. His research interests include nonlinear circuits and systems, with an emphasis on the qualitative analysis and stability of circuits modeling artificial neural networks. His research activity also includes aspects of electromagnetic compatibility. He served as an Associate Editor for IEEE Transactions on Circuits and Systems—I: Fundamental Theory and Applications, from 2001 to 2003, and IEEE Transactions on Neural Networks and Learning Systems, from 2001 to 2010. Since 2016, he has been serving as an Associate Editor for IEEE Transactions on Cybernetics. Since 2024, he has been serving as the Co-Editor-in-Chief for *Neural Networks* (Elsevier).

LUCA PANCIONI received the Laurea degree in telecommunication engineering and the Ph.D. degree in information engineering from the University of Siena, Siena, Italy, in 2001 and 2004, respectively. He is currently an Assistant Professor of electrical engineering with the Department of Information Engineering and Mathematics, University of Siena. His research interests include analysis of nonlinear circuits modeling neural networks, mainly focused on stability and complex dynamics. Recent activities concern the study and the modeling of neural circuits, including memristors. His research activity also includes modeling of source-coupled logic and electronic design of integrated analog and mixed signals.

GIACOMO INNOCENTI received the master's degree in information engineering and the Ph.D. degree in nonlinear dynamics and complex systems from the University of Florence, Florence, Italy, in 2004 and 2008, respectively. He was a Postdoctoral Research Fellow, first with the University of Florence and then with the University of Siena, Siena, Italy, from 2008 to 2010. Since 2012, he has been an Assistant Professor of automation with the University of Florence, where he is currently with the Department of Information Engineering. His research interests include nonlinear dynamics with particular interest in networks of interacting agents and neuron models. He serves as an Associate Editor for *Scientific* journals in the field of the analysis of nonlinear systems, and he was on the committees of workshops and scientific congresses on the same subject.

ALBERTO TESI received the Laurea degree in electronics engineering from the University of Florence, in 1984, and the Ph.D. degree in systems engineering from the University of Bologna, in 1989. In 1990, he joined the Department of Systems and Computer Science, University of Florence, as a Research Assistant. He is currently a Professor of control systems with the Department of Information Engineering, University of Florence. He is the co-author of about 180 scientific publications. His research interests include analysis of nonlinear dynamics of complex systems, robust control of linear systems, and optimization. He was a member of the Conference Editorial Board of the Conference on Decision and Control from 1994 to 1999 and American Control Conference from 1995 to 2000 and a member of the program committee of several international conferences. He was an Associate Editor of IEEE Transactions on Circuits and Systems—I: Regular Papers, from 1994 to 1995, IEEE Transactions on Automatic Control, from 1995 to 1998, and *Systems and Control Letters*, from 1995 to 2010.

Open Access funding provided by 'Università degli Studi di Siena' within the CRUI CARE Agreement